Available online at www.sciencedirect.com
ScienceDirect
Solid State Nuclear Magnetic Resonance 32 (2007) 16–23
Solid State Nuclear Magnetic Resonance
www.elsevier.com/locate/ssnmr

# A computational investigation of $^{17}O$ quadrupolar coupling parameters and structure in α-quartz phase $GeO_2$

Travis H. Sefzik, Ted M. Clark, Philip J. Grandinetti*

*Department of Chemistry, The Ohio State University, 120 W. 18th Avenue, Columbus, OH 43210-1173, USA*

Received 12 March 2007; received in revised form 4 June 2007
Available online 10 July 2007

**Abstract**

*Ab initio* band-structure calculations based on density functional theory have been completed for α-quartz phase $GeO_2$ to obtain electric-field gradients (efg) for oxygen atoms, including those for $GeO_2$ at elevated pressure and temperature. To interpret the resulting efg values and examine correlations between structure and $^{17}O$ quadrupolar coupling parameters, additional *ab initio* self-consistent Hartree-Fock molecular orbital calculations were completed. The quadrupolar coupling constant was found to have a strong dependence on Ge–O distance and ∠Ge−O−Ge, with the quadrupolar asymmetry parameter being primarily dependent on ∠Ge−O−Ge. Analytical expressions describing these dependencies consistent with earlier investigations of analogous silicate compounds are also reported.


## 1. Introduction

Germanate compounds, including α-quartz phase $GeO_2$, are of interest to a wide range of researchers in several disciplines because they serve as an experimental proxy for silicate systems of fundamental importance. The compression behavior of $GeO_2$ largely parallels that of $SiO_2$, but at pressures much more easily attained experimentally [1,2]. Crystalline germanates have been investigated by a variety of methods [1,3–5], including a more recent determination of the crystal structure of α-quartz phase $GeO_2$ as a function of pressure [6]. Amorphous germanates have also been investigated by a variety of methods [2,4,7–13]. Recent neutron and X-ray diffraction studies of ambient and permanently densified germania glass concluded that a decrease in Ge–O and O–O distances occurs upon densification, caused by a rotation about the Ge–O–Ge bonds and a distortion of the $GeO_4$ tetrahedra [14].

In spite of these recent successes, improved methods are still needed to resolve a number of outstanding questions about structural variations in tetrahedral oxides glasses. An experimental approach that has great potential for describing bridging oxygen environments in both crystalline and amorphous materials is $^{17}O$ solid-state nuclear magnetic resonance (NMR) spectroscopy. Advances in solid-state NMR have led to a significant increase in the number of bridging oxygen environments with experimentally determined NMR parameters [15–20]. The relationships between structure and the $^{17}O$ NMR parameters in tetrahedral oxides have been an area of focus for some time [21–26]. First coordination sphere features of the bridging oxygen site, such as the ∠T−O−T and T–O bond distance, have been studied and analytical expressions proposed to predict the nuclear electric quadrupolar coupling constant ($C_q$) and asymmetry parameter ($\eta_q$). Such relationships have been indispensable for interpreting $^{17}O$ NMR data obtained for amorphous silicates [15,27,28].

Unfortunately, unlike the situation for crystalline silicates [29–34], there is only one experimental measurement of $^{17}O$ nuclear electric quadrupolar coupling parameters in a crystalline germanate with a Ge–O–Ge linkage [20]. Therefore, in this work we have focused on predicting the quadrupolar coupling parameters of germanate bridging oxygen by combining *ab initio* computational approaches that incorporate crystal periodicity [35,36] with those that utilize model clusters to represent the salient features in the local environment [16,36–42]. As we have shown earlier [23], there are advantages for employing both approaches when determining trends in quadrupolar

*Corresponding author. Fax: +1 614 292 1685.
*E-mail address:* grandinetti.1@osu.edu (P.J. Grandinetti).

0926-2040/$ - see front matter © 2007 Elsevier Inc. All rights reserved.
doi:10.1016/j.ssnmr.2007.07.002

couplings for oxygen sites. In this investigation we concentrate on calculations of the $^{17}O$ quadrupolar coupling parameters for crystal structures determined for quartz-type $GeO_2$ at elevated pressures and temperatures. Previously reported trends [22] between structural parameters, such as ∠T−O−T or T–O distance, are also considered and are discussed with respect to trends reported for similar silicate environments.

## 2. Calculations

The efg tensor components are related to the quadrupolar coupling constant ($C_q$) and quadrupolar asymmetry parameter ($\eta_q$) according to

$$C_q = eQ_I\langle eq_{zz}\rangle/h, \tag{1}$$

and

$$\eta_q = \frac{\langle eq_{xx}\rangle - \langle eq_{yy}\rangle}{\langle eq_{zz}\rangle}, \tag{2}$$

where $Q$ is the nuclear electric quadrupole moment and $\langle eq_{xx}\rangle$, $\langle eq_{yy}\rangle$, and $\langle eq_{zz}\rangle$ are the principal components of the traceless efg tensor defined such that $|\langle eq_{zz}\rangle| > |\langle eq_{yy}\rangle| > |\langle eq_{xx}\rangle|$.

### 2.1. Periodic structure calculations

The full-potential, linearized, augmented plane-wave (LAPW) package WIEN2k [35] was used to perform density functional theory (DFT) using the generalized gradient approximations (GGA) for the exchange and correlation potentials [43,44]. In the LAPW method the unit cell is divided into spheres centered at the atomic positions and an interstitial region. For the interstitial region, the basis set consists of plane waves which are augmented by atomic-like solutions inside the spheres. Sphere radii of 1.4550 and 1.1640 a.u. were used for Ge and O, respectively. The cutoff for the plane wave basis set was chosen as $R_{mt}K_{max} = 7.00$, where $R_{mt}$ corresponds to the smallest atomic sphere radii and $K_{max}$ is the plane wave cutoff. These parameters typically resulted in more than 6000 LAPWs being used in the basis sets. Additional calculations confirmed that these results were well converged for these cut-off values. The number of $k$-points in the irreducible Brillouin zone (IBZ) for the calculations was consistently 12 throughout the study. Nonspin-polarized calculations were studied in all cases. The procedure for obtaining the electric field gradient tensor with WIEN2k is given in Ref. [36].

### 2.2. Structure fragment calculations

*Ab initio* molecular orbital calculations were performed using the Gaussian 03 [45] software package at a restricted Hartree-Fock level with a 6-311 + $G(d)$ basis set used for all atoms. A value of $e^2Q/h = -6.11$ MHz-au$^3$ was used for $^{17}O$ to convert the largest magnitude principle component of the efg tensor in atomic units to the $^{17}O$ quadrupolar coupling constant in megaHertz.

Bridging oxygen centered fragments, as shown in Fig. 1A, consisting of one tetrahedral shell (1T), $(OH_3)Ge-O-Ge(OH_3)$, were employed for calculation of the electric-field gradient. A select number of two $GeH_3$ terminated tetrahedral shells (2T), $(H_3GeO)_3Ge-O-Ge(OGeH_3)_3$, as shown in Fig. 1B, were also examined. The geometries of the fragments are consistent with the crystal structure determined by neutron diffraction investigations [6,46]. Fragments were terminated either at germanium or oxygen atoms by hydrogen atoms placed along the direction of the Ge–O or O–Ge bond in the actual crystal structure. The O–H and Ge–H bond distances were fixed at 0.96 and 1.52 Å, respectively.

Model 1T clusters were also used to examine trends between structure and quadrupolar coupling parameters $GeO_2$ systems. For these calculations the ∠Ge−O−Ge angle was varied between 125° and 160° in steps of 5°. The

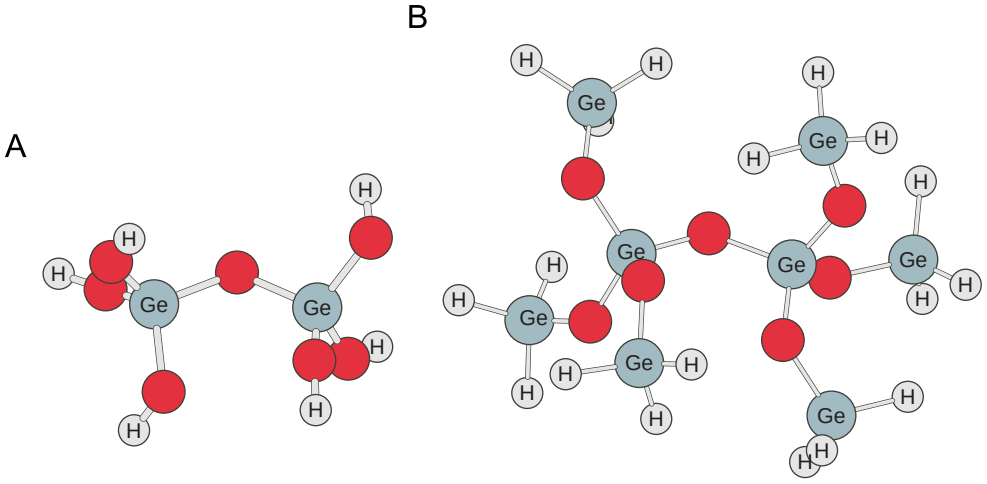


Fig. 1. Oxygen centered crystal fragments for quartz-type $GeO_2$. The one tetrahedral shell (1T), and two tetrahedral shell (2T) fragments, depicted in (A) and (B), respectively, are based on the crystal structure for ambient $GeO_2$.

central Ge–O distances were varied between 1.70 and 1.75 Å in 0.01 Å increments for each of these angles. Both symmetric and asymmetric distance pairs were examined.

## 3. Results and discussion

### 3.1. Structures

Crystal structures have been reported for quartz-type $GeO_2$ under different conditions. High pressure $GeO_2$ crystal structures, based on a neutron diffraction study, have been reported by Glinnemann [6]. A series of crystal structures has also been reported by Haines [46] for $GeO_2$ as a function of temperature, again based on neutron diffraction data. Structure refinements for $GeO_2$ under ambient pressure and temperature conditions have been reported by Smith [49] and Sowa [50]. All of these studies are in good agreement with respect to the ambient $GeO_2$ structure with a $\angle$Ge−O−Ge value of 130.1°, asymmetric Ge–O distances of 1.737 and 1.741 Å, and tetrahedral O–Ge–O angles of ranging from 106.3° to 113.1°.

The structural changes that occur in quartz-type $GeO_2$ with temperature or pressure changes are shown in Fig. 2. The response of crystalline α-quartz phase $SiO_2$ to changes in these two variables is also included for comparison [47,48]. As shown in Fig. 2A, the trend in $\angle$T−O−T (where T = Ge or Si) is similar for both $GeO_2$ and $SiO_2$, with the angle contracting as the unit cell volume decreases. It should be noted, however, that considerably higher pressures are required to compress the unit cell for $SiO_2$ in comparison to $GeO_2$. For example, the unit cell volume of $SiO_2$ is decreased from approximately 113 to 100 Å$^3$ with a pressure change of 61.4 kbar. In comparison, the unit cell volume of $GeO_2$ is decreased from approximately 121 to 108 Å$^3$ with a much smaller pressure change of 5.57 GPa. In terms of unit cell expansion as a function of temperature the response of each system are similar; the unit cell volumes increase by approximately 5 Å$^3$ for $SiO_2$ or $GeO_2$ with a temperature increase of 1000 K.

Similar trends are also apparent for T–O distance as a function of unit cell volume shown in Fig. 2B. The unit cell expands as the temperature is increased and the T–O distances decrease by approximately 0.01–0.02 Åwhen the temperature is increased to approximately 1300 K in comparison to the ambient structure. With unit cell contraction the T–O distances are largely unchanged with respect to the ambient structure. Finally, the relationship between $\angle$T−O−T and T–O distance, shown in Fig. 2C, are similar for both $GeO_2$ and $SiO_2$. A negative correlation between angle and distance is present as the unit cell volume increases with rising temperature, i.e., the bridging oxygen angle decreases and the T–O distance increases. In contrast, a clear negative correlation is not apparent for the compressed unit cell structures for either $GeO_2$ or $SiO_2$.

### 3.2. Calculation of quadrupolar coupling parameters

Using the reported α-quartz $GeO_2$ crystal structures of Glinnemann [6] as a function of pressure and Haines [46] as a function of temperature, the quadrupolar coupling parameters in Table 1 were calculated for the bridging oxygen. One set of calculations were performed on the full crystal lattice structures using the periodic DFT methods in WIEN2k, and another on the 1T fragments using Gaussian 03. The $C_q$ and $\eta_q$ values obtained are shown in Table 1. The WIEN2k values for the ambient crystal structure are in reasonable agreement with the experimental values reported by Dupree and co-workers [19] of $C_q = 7.3 \pm 0.1$ MHz and $\eta_q = 0.48 \pm 0.05$ as determined by NMR. This agreement is not surprising given the effectiveness of LAPW calculations for similar systems [23,36,51]. The $C_q$ values calculated for 1T fragments, also shown in Table 1,

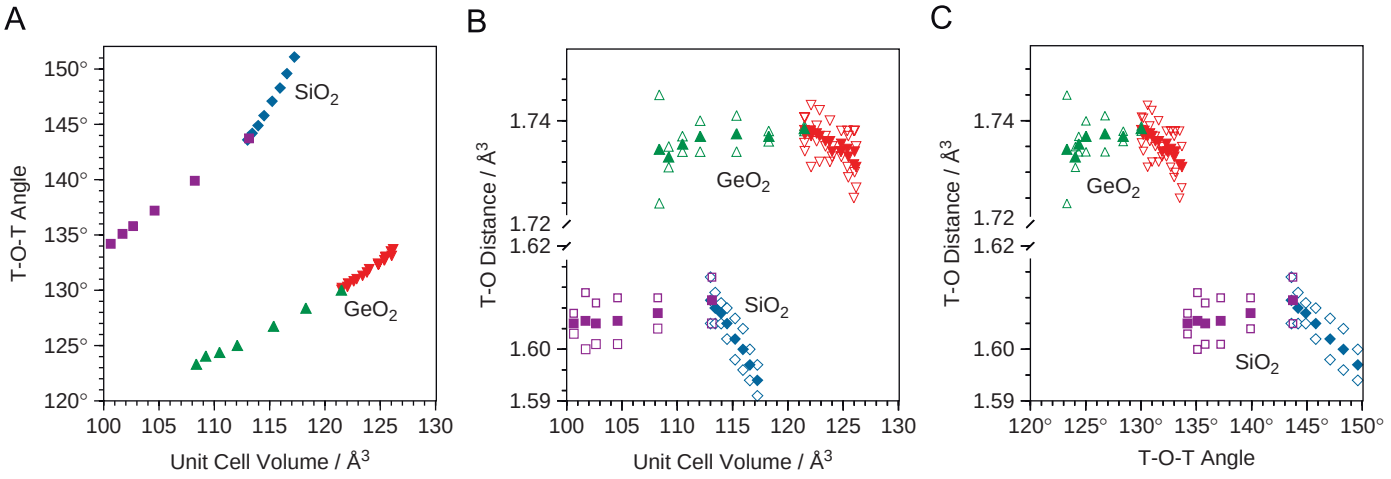


Fig. 2. Reported structural distributions in quartz-type $SiO_2$ and $GeO_2$. (A) T–O–T angle as a function of unit cell volume, (B) T–O distance as a function of unit cell volume, and (C) T–O distance as a function of $\angle$T−O−T. Values are based on crystal structure determinations for $SiO_2$ (square symbol: temperature dependence at constant pressure [47] and diamond symbol: pressure dependence at constant temperature [48]), and $GeO_2$ (triangle symbol: temperature dependence at constant pressure [6] and inverted triangle symbol: pressure dependence at constant temperature [46]). Average T–O distance values are shown as filled symbols.

Table 1
Reported structural parameters and calculated quadrupolar coupling constants and asymmetry parameters (this study) at oxygen sites in quartz-type $GeO_2$ at various pressure [6] and temperature [46] conditions

| Press. (GPa) | Temp. (K) | ∠Ge−O−Ge (°) | $d$(Ge−O) (Å) | ∠O−Ge−O (°) | LAPW | | 1T Fragment | | $C_q$ ratio |
|---|---|---|---|---|---|---|---|---|---|
| | | | | | $C_q$ (MHz) | $\eta_q$ | $C_q$ (MHz) | $\eta_q$ | |
| 5.57 | – | 123.4 | 1.724, 1.745 | 103.5, 108.1, 110.0, 116.1 | −6.79 | 0.73 | −7.06 | 0.65 | 0.962 |
| 5.12 | – | 124.0 | 1.731, 1.735 | 104.1, 107.9, 109.3, 116.0 | −6.79 | 0.72 | −7.08 | 0.64 | 0.959 |
| 4.53 | – | 124.3 | 1.734, 1.737 | 104.1, 108.0, 110.0, 115.5 | −6.85 | 0.71 | −7.16 | 0.63 | 0.957 |
| 3.74 | – | 125.0 | 1.734, 1.740 | 104.6, 107.8, 110.1, 115.0 | −6.91 | 0.69 | −7.23 | 0.62 | 0.956 |
| 2.18 | – | 126.8 | 1.734, 1.741 | 105.3, 107.5, 110.0, 114.5 | −7.04 | 0.65 | −7.41 | 0.58 | 0.950 |
| 1.07 | – | 128.4 | 1.736, 1.738 | 105.7, 107.6, 110.3, 113.2 | −7.15 | 0.60 | −7.59 | 0.54 | 0.942 |
| 0.0001 | – | 130.04 | 1.738, 1.739 | 106.3, 107.6, 110.3, 113.2 | −7.30 | 0.55 | −7.77 | 0.51 | 0.940 |
| – | 294 | 130.2 | 1.734, 1.741 | 106.3, 107.9, 110.5, 113.0 | −7.29 | 0.55 | −7.77 | 0.50 | 0.938 |
| – | 298 | 130.1 | 1.736, 1.741 | 106.3, 107.7, 110.5, 113.0 | −7.28 | 0.56 | −7.77 | 0.51 | 0.937 |
| – | 425 | 130.3 | 1.738, 1.738 | 106.4, 107.4, 110.5, 113.1 | −7.29 | 0.55 | −7.78 | 0.51 | 0.937 |
| – | 449 | 130.6 | 1.731, 1.743 | 106.4, 108.2, 111.0, 112.4 | −7.32 | 0.53 | −7.81 | 0.49 | 0.937 |
| – | 571 | 130.8 | 1.736, 1.739 | 106.6, 107.5, 110.4, 113.0 | −7.33 | 0.54 | −7.82 | 0.50 | 0.937 |
| – | 634 | 131.0 | 1.732, 1.742 | 106.6, 108.0, 111.1, 112.4 | −7.34 | 0.53 | −7.85 | 0.48 | 0.935 |
| – | 756 | 131.3 | 1.735, 1.737 | 106.7, 107.3, 110.4, 112.9 | −7.36 | 0.53 | −7.86 | 0.49 | 0.936 |
| – | 845 | 131.6 | 1.732, 1.740 | 106.7, 107.8, 111.1, 112.3 | −7.39 | 0.51 | −7.89 | 0.47 | 0.937 |
| – | 890 | 131.9 | 1.733, 1.735 | 106.9, 107.2, 110.3, 112.8 | −7.38 | 0.51 | −7.88 | 0.48 | 0.937 |
| – | 1043 | 132.4 | 1.734, 1.734 | 106.9, 107.2, 110.3, 112.7 | −7.41 | 0.51 | −7.92 | 0.47 | 0.936 |
| – | 1059 | 132.3 | 1.733, 1.738 | 107.1, 107.3, 110.3, 112.5 | −7.43 | 0.51 | −7.95 | 0.47 | 0.935 |
| – | 1175 | 132.7 | 1.731, 1.738 | 106.9, 107.3, 110.0, 112.7 | −7.44 | 0.50 | −7.95 | 0.46 | 0.936 |
| – | 1215 | 133.0 | 1.729, 1.737 | 106.7, 107.4, 109.5, 112.9 | −7.43 | 0.50 | −7.96 | 0.46 | 0.933 |
| – | 1275 | 133.1 | 1.730, 1.738 | 106.1, 107.7, 109.5, 113.0 | −7.45 | 0.50 | −7.97 | 0.47 | 0.935 |
| – | 1298 | 133.5 | 1.725, 1.738 | 106.7, 107.6, 109.8, 112.6 | −7.45 | 0.48 | −7.98 | 0.45 | 0.934 |
| – | 1344 | 133.7 | 1.727, 1.735 | 106.4, 107.7, 109.4, 112.9 | −7.46 | 0.48 | −7.98 | 0.45 | 0.935 |

The first-coordination sphere geometry of 1T fragments were taken from the crystal structure. The last column is the ratio of the $C_q$ values for LAPW calculation over the 1T fragment calculation.

are consistently larger in magnitude than the LAPW calculated values or the experimentally determined value for α-quartz $GeO_2$ under ambient conditions. This finding is consistent with previous investigations utilizing *ab initio* methods [22,23,33]. Our results suggest that, for the 1T fragments and calculation performed at a restricted Hartree-Fock level with a 6-311 + $G(d)$ basis set used for all atoms, an efg scaling factor of 0.94 is needed to obtain a more accurate $C_q$ value. Since $\eta_q$ values are calculated as a ratio of efg principal components, their values should, in principle, be unaffected by a need for efg scaling. Both approaches give $\eta_q$ values in good agreement with experiment, however, $\eta_q$ values obtained with the MO-cluster approach are slightly better in agreement than those from the LAPW method.

Additional calculations were performed with larger 2T fragments. These results were similar to those obtained using 1T fragments, e.g., parameters calculated for the ambient structure were $C_q = 7.65$ MHz and $\eta_q = 0.46$. As before, $C_q$ values required an efg scaling for better agreement with WIEN2k and experiment. This suggests that the efg is partially dependent on the fragment size employed in a given calculation. The $\eta_q$ value obtained using the 2T fragment is slightly smaller than that obtained for the 1T fragment, and also in better agreement with experiment. These findings are consistent with previous investigations of analogous silicate environments which demonstrated that 1T-fragment are sufficient for determining the quadrupolar coupling parameters of a bridging oxygen atom [52], and a prudent choice given the significantly longer time required to complete 2T fragment calculations.

Having demonstrated that *ab initio* molecular orbital calculations employing oxygen centered 1T fragments are suitable for determining the quadrupolar coupling parameters in these germanate systems, it is now possible to examine which structural features in the first coordination sphere most affect the efg. Earlier investigations have identified several factors that may influence the efg at bridging oxygen sites in germanate, silicate, or other related compounds [23,25,26]. This prior work strongly suggests that $C_q$ will be affected by changes in both ∠Ge−O−Ge and Ge–O distance, with variations in ∠O−Ge−O being a secondary factor. It is also expected that $\eta_q$ will be affected by changes in ∠Ge−O−Ge, with other contributions in the first coordination sphere being of minor importance.

To examine these hypotheses, 1T models were constructed and the efg-components calculated. By systematically varying the ∠Ge−O−Ge and Ge–O distances it is possible to compute quadrupolar coupling parameters for structures with far greater first-coordination sphere variability than that present in reported crystal structures. In Fig. 3 are the predicted trends in $C_q$ and $\eta_q$ as both ∠Ge−O−Ge and Ge–O distance are independently varied.

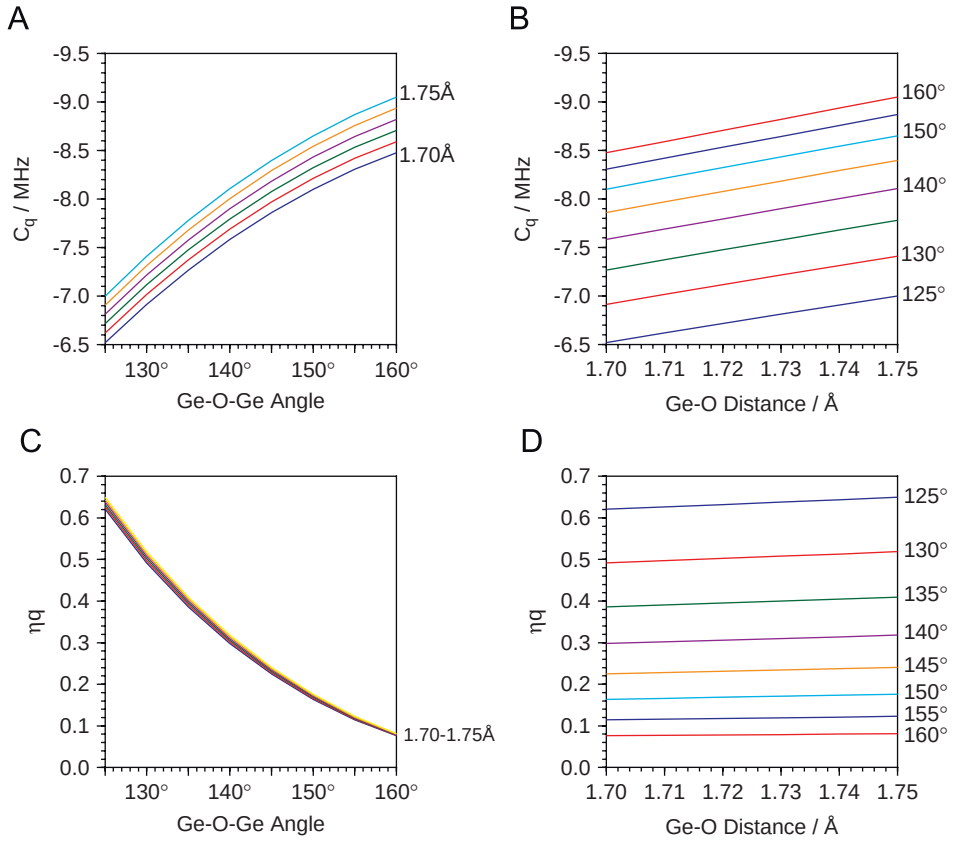


Fig. 3. Trends in MO-cluster calculated $C_q$ (efg scaled) and $\eta_q$ parameters as a function of angle and distance in $(OH)_3$ Ge–O–Ge$(OH)_3$ clusters. (A) Quadrupolar coupling constant, and (B) quadrupolar asymmetry parameter for ∠Ge−O−Ge ranging from 125° to 160° in 5° increments. (C) Quadrupolar coupling constant and (D) quadrupolar asymmetry parameter for Ge–O distances ranging from 1.70–1.75 Å in 0.01 Å increments.

Other than the magnitude of $C_q$, these trends are virtually identical to those described earlier by Clark and Grandinetti for the Si–O–Si linkage [22]. Over the relevant range of Ge–O distances the $C_q$ value follows a simple linear relationship [26]. Most importantly, the asymmetry parameter is nearly independent of Ge–O distance, and its behavior is dominated by its dependence on ∠Ge−O−Ge. These trends can be described using the same expressions used for the Si–O–Si linkage [26]:

$$C_q(d_{TO},\Omega) = a\left(\frac{1}{2}+\frac{\cos\Omega}{\cos\Omega-1}\right)^{\alpha} + m_d(d_{TO}-d_{TO}^{\circ}), \qquad (3)$$

and

$$\eta_q(\Omega) = b\left(\frac{1}{2}-\frac{\cos\Omega}{\cos\Omega-1}\right)^{\beta}, \qquad (4)$$

where $\Omega$ is ∠Ge−O−Ge and $d_{TO}$ is the average germanium-oxygen bond distance. The parameters obtained from fitting the theoretical data to Eqs. (3) and (4) are $a = -6.1$ MHz, $m_d = -10.60$ MHz/Å, $d_{TO}^{\circ} = 1.449$ Å, $\alpha = 4.58$, $b = 3.22$, and $\beta = 0.992$.

As a check we used the quadrupolar coupling parameters predicted in our periodic structure calculations for α-$GeO_2$, LAPW in Table 1, and Eqs. (3) and (4) to back predict the Ge–O–Ge angles and Ge–O distances. This comparison is shown in Fig. 4. The nearly perfect correlation in Fig. 4A shows, as was the case for the Si–O–Si linkage, that the $\eta_q$ value serves as a highly reliable probe of the ∠T−O−T. With ∠Ge−O−Ge determined by $\eta_q$, Eq. (3) is used to predict the Ge–O distance from $C_q$, as shown in Fig. 4B. The predicted Ge–O distances are also in good agreement, with the majority being within 0.005 Å from the predicted value. Having determined the Ge–O distance for a given angle, it is also possible to determine the Ge–Ge distance. These values are shown Fig. 4C. Finally, we note that the simultaneous measurement of $C_q$ and $\eta_q$ for each bridging oxygen site can be exploited to obtain the correlation between Ge–O–Ge angle and Ge–O distance [2,22].

Previous investigations of the relationship between structure and quadrupolar coupling parameters, e.g., in silicate systems, have focused primarily on symmetric T–O bond distances at bridging oxygen sites. Although this assumption is justified since Si–O bonds are typically quite symmetric for a given oxygen site in most crystalline $SiO_2$ polymorphs, with germanates such an assumption is less valid. As seen in Table 1, it is not unusual to have Ge–O distances differ by 0.01 Å at an oxygen site. To examine the effect such structural asymmetries may have on $C_q$ and $\eta_q$, additional calculations have been completed on 1T model clusters with asymmetric Ge–O bond lengths. These calculations, in which asymmetries of up to 0.05 Å were

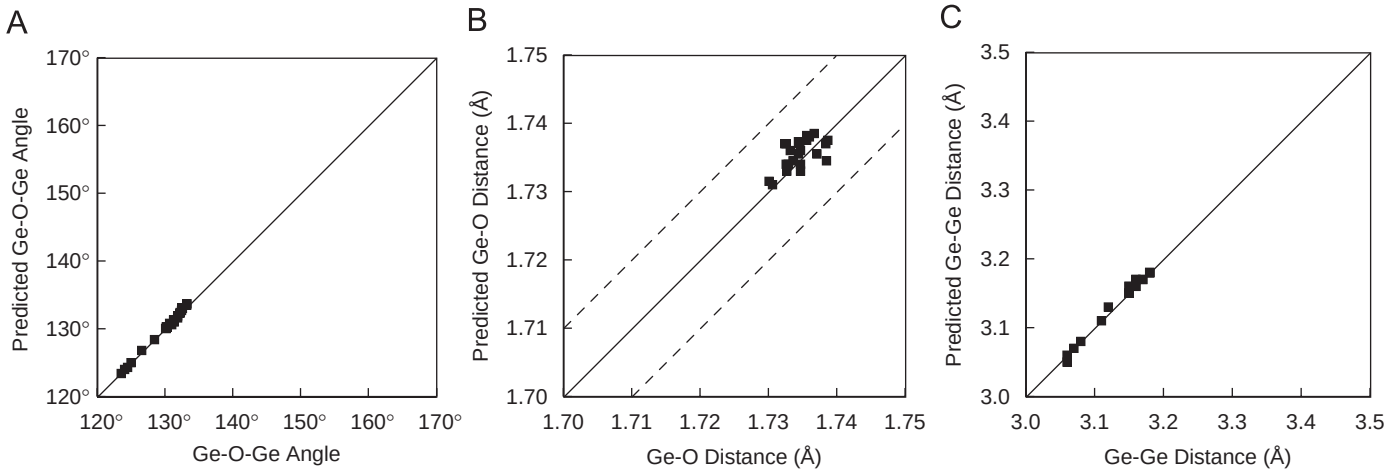


Fig. 4. Comparison of (A) Ge–O–Ge angles, (B) Ge–O distances, and (C) Ge–Ge distances predicted with Eqs. (3) and (4) using the LAPW (Table 1) predicted $^{17}$O Quadrupolar Coupling parameters of α-$GeO_2$ with corresponding quantities reported from structure for α-$GeO_2$. Solid diagonal lines represent perfect agreement. Best fit parameters for Eqs. (3) and (4) are $a = -6.1$ MHz, $m_d = -10.60$ MHz/Å, $d^{\circ}_{TO} = 1.449$ Å, $\alpha = 4.58$, $b = 3.22$, and $\beta = 0.992$.

considered, strongly suggest that the *average* T–O distance, as included in Eq. (3), remains very useful for describing even asymmetric bridging oxygen environments. For example, 1T-clusters with ∠Ge−O−Ge = 135° and Ge–O distances pairs of 1.73–1.73, 1.74–1.72, and 1.75−1.71 Å (average $d$(Ge−O) = 1.73 Å) have calculated $C_q$ values of 7.51, 7.51, and 7.52 MHz, respectively. The calculated $\eta_q$ are even less varied, with a value of 0.40 determined for each cluster. Although it remains possible that other asymmetric features further removed from a bridging oxygen atom, such as varied ∠O−Ge−O, may complicate the relationships between structure and quadrupolar coupling parameters in germanates, vis-à-vis silicates, Eqs. (3) and (4) should remain valid for a wide range of germanate structures.

## 4. Conclusion

General trends in the $^{17}$O quadrupolar coupling parameters for bridging oxgyen atoms in germanates have been described based on *ab initio* self-consistent field Hartree-Fock molecular orbital calculations on germanate clusters. These results were calibrated by performing band-structure calculations based on the density functional theory for a range of α-quartz phase $GeO_2$ structures obtained as a function of pressure [6] and temperature [46]. As suggested by earlier investigations, the quadrupolar asymmetry parameter was found to be primarily dependent on the ∠Ge−O−Ge (and largely independent of Ge–O distance). The quadrupolar coupling constant was found to have a strong dependence on Ge–O distance, as well as ∠Ge−O−Ge. Having established the manner in which local structural parameters influence the $^{17}$O quadrupolar coupling parameters, it is now possible to gain significant insights into the structure of germanate glasses. Since the relationships between structure and the $^{17}$O quadrupolar coupling parameters appear similar for both germanate and silicate systems, future work describing correlated structural distributions in $GeO_2$ glasses should be possible, as has been recently reported for silica glass [15].

## Acknowledgments

This material is based upon work supported by the National Science Foundation under Grants CHE-0616881 and Le Studium (Orléans, France). Any opinions, findings and conclusions or recommendations expressed in this material are those of the author(s) and do not necessarily reflect the views of the National Science Foundation. We would also like to thank Dr. Wendy Panero of the Ohio State University's Geology Department for her assistance with interpreting diffraction results.

## References

[1] J.P. Itie, A. Polian, G. Calas, J. Petiau, A. Fontaine, H. Tolentino, Pressure induced coordination changes in crystalline and vitreous $GeO_2$, Phys. Rev. Lett. 63 (4) (1989) 398–401.
[2] D.J. Durben, G.H. Wolf, Raman spectroscopic study of the pressure-induced coordination change in $GeO_2$ glass, Phys. Rev. B 43 (3) (1991) 2355–2363.
[3] W.H. Baur, A.A. Khan, Rutile-type compounds. IV. $SiO_2$, $GeO_2$ and a comparison with other rutile-type structures, Acta Cryst. B 27 (1971) 2133–2139.
[4] B. Houser, N. Alberding, R. Ingalls, E.D. Crozier, High pressure study of alpha-quartz $GeO_2$ using extended X-ray absorption fine structure, Phys. Rev. B 37 (11) (1988) 6513–6516.
[5] J.D. Jorgensen, Compression mechanisms in α-quartz structures — $SiO_2$ and $GeO_2$, J. Appl. Phys. 49 (1978) 5473.
[6] J. Glinnemann, H.E. King, H. Schulz, T. Hahn, S.J. LaPlaca, F. Dacol, Crystal-structures of the low-temperature quartz-type phases of $SiO_2$ and $GeO_2$ at elevated pressure, Z. Kristallogr. 198 (3 & 4) (1992) 177–212.

[7] P.V. Teredesai, D.T. Anderson, N. Hauser, K. Lantzky, J.L. Yarger, Infrared spectroscopy of germanium dioxide ($GeO_2$) glass at high pressure, Phys. Chem. Glasses 46 (4) (2005) 345–349.
[8] M. Okuno, C.D. Yin, H. Morikawa, F. Marumo, A high resolution EXAFS and near edge study of $GeO_2$ glass, J. Non Cryst. Solids 87 (1986) 312.
[9] Y. Yashiro, A. Yoshiasa, O. Kamishima, T. Tsuchiya, T. Yamanaka, T. Ishii, H. Maeda, Exafs study on the anharmonic effective pair potential in rutile type alpha-quartz type, and vitreous $GeO_2$, J. Phys. IV 7 (C2) (1997) 1175–1176.
[10] S. Kawasaki, XAFS study of pressure-amorphized $GeO_2$, J. Mater. Sci. Lett. 15 (21) (1996) 1860–1862.
[11] S. Sugai, A. Onodera, Medium-range order in permanently densified $SiO_2$ and $GeO_2$ glass, Phys. Rev. Lett. 77 (20) (1996) 4210–4213.
[12] R.J. Hemley, C. Meade, H.K. Mao, Comment on "Medium-range order in permanently densified $SiO_2$ and $GeO_2$ glass," Phys. Rev. Lett. 79 (7) (1997) 1420.
[13] A.S. Zyubin, O.A. Kondakova, S.A. Dembovsky, Quantum-chemical simulations of the transformations of continuous random network in the vitreous $GeO_2$, Glass Phys. Chem. 23 (1997) 58.
[14] S. Sampath, C.J. Benmore, K.M. Lantzky, J. Neuefeind, K. Leinenweber, D.L. Price, J.L. Yarger, Intermediate-range order in permanently densified $GeO_2$ glass, Phys. Rev. Lett. 90 (11) (2003) 115502.
[15] T.M. Clark, P.J. Grandinetti, P. Florian, J.F. Stebbins, Correlated structural distributions in silica glass, Phys. Rev. B 70 (6) (2004) 064202.
[16] T.M. Alam, J.M. Segall, Structural perturbations on the bridging oxygen $^{17}O$ NMR EFG parameters in ultraphosphates: an ab initio study, J. Mol. Structure Theochem 674 (1–3) (2004) 167–175.
[17] R.T. Hart, Zwanziger, $^{17}O$ NMR spectroscopy of $\alpha$-$TeO_2$ and $Na_2TeO_3$, J. Am. Ceram. Soc. 88 (8) (2005) 2325–2327.
[18] R.T. Hart, J.W. Zwanziger, U. Werner-Zwanziger, Y.R. Yates, On the spectral similarity of bridging and nonbridging oxygen in tellurites, J. Phys. Chem. A 109 (33) (2005) 7636–7641.
[19] R. Hussin, R. Dupree, D. Holland, The Ge–O–Ge bond angle distribution in $GeO_2$ glass: a NMR determination, J. Non Cryst. Solids 246 (3) (1999) 159–246.
[20] R. Hussin, D. Holland, R. Dupree, Does six-coordinate germanium exist in $Na_2O-GeO_2$ glasses? Oxygen-17 nuclear magnetic resonance measurements, J. Non Cryst. Solids 232–234 (1998) 440–445.
[21] J.A. Tossell, P. Lazzeretti, *Ab Initio* calculations of oxygen nuclear quadrupolar coupling constants and oxygen and silicon NMR shielding constants in molecules containing Si–O bonds, Chem. Phys. Lett. 112 (1987) 205.
[22] T.M. Clark, P.J. Grandinetti, Dependence of bridging oxygen $^{17}O$ quadrupolar coupling parameters on Si–O distance and Si–O–Si angle, J. Phys. Condens. Mater. 15 (31) (2003) S2387–S2395.
[23] T.M. Clark, P.J. Grandinetti, Calculation of bridging oxygen $^{17}O$ quadrupolar coupling parameters in alkali silicates: a combined ab initio investigation, Solid State NMR 27 (2005) 233–241.
[24] J.A. Tossell, Calculation of $^{17}O$ NMR shieldings in molecular models for crystalline MO, M = Mg, Ca, Sr, and in models for alkaline earth silicates, Phys. Chem. Miner. 31 (1) (2004) 41–44.
[25] T.M. Clark, P.J. Grandinetti, Relationships between bridging oxygen $^{17}O$ quadrupolar coupling parameters and structure in germanates, J. Non Cryst. Solids 265 (2000) 75–82.
[26] T.M. Clark, P.J. Grandinetti, Factors influencing the $^{17}O$ quadrupole coupling constant in bridging oxygen environments, Solid State NMR 16 (2000) 55–62.
[27] I. Farnan, P.J. Grandinetti, J.H. Baltisberger, J.F. Stebbins, U. Werner, M.A. Eastman, A. Pines, Quantification of the disorder in network-modified silicate glasses, Nature 358 (1992) 31–35.
[28] S.K. Lee, Structure of silicate glasses and melts at high pressure: quantum chemical calculations and solid-state NMR, J. Phys. Chem. B 108 (19) (2004) 5889–5900.
[29] H.K.C. Timken, N. Janes, G.L. Turner, S.L. Lambert, L.B. Welsh, E. Oldfield, Solid-state oxygen-17 nuclear magnetic resonance spectroscopic studies of zeolites and related systems, J. Am. Chem. Soc. 108 (1986) 7236.
[30] H.K.C. Timken, S.E. Schramm, R.J. Kirkpatrick, E. Oldfield, Solid-state oxygen-17 nuclear magnetic resonance spectroscopic studies of alkaline earth metasillicates, J. Phys. Chem. 91 (1987) 1054–1058.
[31] P.J. Grandinetti, J.H. Baltisberger, U. Werner, A. Pines, I. Farnan, J.F. Stebbins, Solid-state $^{17}O$ magic-angle and dynamic-angle spinning NMR study of coesite, J. Phys. Chem. 99 (1995) 12341–12348.
[32] L.M. Bull, B. Bussemer, T. Anupold, A. Reinhold, A. Samoson, J. Sauer, A.K. Cheetham, R. Dupree, A high-resolution $^{17}O$ and $^{29}Si$ NMR study of zeolite siliceous ferrierite and ab initio calculations of NMR parameters, J. Am. Chem. Soc. 122 (2000) 4948–4958.
[33] T.M. Clark, P.J. Grandinetti, P. Florian, J.F. Stebbins, An $^{17}O$ NMR investigation of crystalline sodium metasilicate: implications for the determinations of local structure in alkali silicates, J. Phys. Chem. B 105 (2001) 12257–12265.
[34] D.R. Spearing, I. Farnan, J.F. Stebbins, Dynamics of the alpha-beta phase transitions in quartz and cristobalite as observed by in situ high temperature Si-29 NMR and $^{17}O$ NMR, Phys. Chem. Min. 19 (5) (1992) 307–321.
[35] P. Blaha, K. Schwarz, G.K.H. Madsen, D. Kvasnicka, J. Luitz, WIEN2k, an augmented plane wave plus local orbitals program for calculating crystal properties (2001).
[36] B. Winkler, P. Blaha, K. Schwarz, Ab initio calculation of electric-field gradient tensors of forsterite, Am. Mineral. 81 (5 & 6) (1996) 545–549.
[37] E.K. Yildirim, R. Dupree, Study of the relationship between structure and $^{17}O$ electric field gradient parameters in some aluminosilicates, Modern Phys. Lett. B 19 (24) (2005) 1213–1221.
[38] T. Charpentier, S. Ispas, M. Profeta, F. Mauri, C.J. Pickard, First-principles calculation of the $^{17}O$, $^{29}Si$, and $^{23}Na$ spectra of sodium silicate crystals and glasses, J. Phys. Chem. B 108 (13) (2004) 4147–4161.
[39] M. Profeta, F. Mauri, C.J. Pickard, Accurate first principles prediction of $^{17}O$ NMR parameters in $SiO_2$: assignment of the zeolite ferrierite spectrum, J. Am. Chem. Soc. 125 (2003) 541–548.
[40] C. Gervais, R. Dupree, K.J. Pike, C. Bonhomme, M. Profeta, C.J. Pickard, F. Mauri, Combined first-principles computational and experimental multinuclear solid-state NMR investigation of amino acids, J. Phys. Chem. A 109 (31) (2005) 6960–6969.
[41] M. Benoit, M. Profeta, F. Mauri, C.J. Pickard, M.E. Tuckerman, First-principles calculation of the $^{17}O$ NMR parameters of a calcium aluminosilicate glass, J. Phys. Chem. B 109 (13) (2005) 6052–6060.
[42] S. Sen, C.A. Russell, Point-charge calculations of quadrupolar parameters for bridging oxygen sites in vitreous silica: structural implications, Phys. Rev. B 72 (17) (2005) 174205.
[43] J.P. Perdew, K. Burke, M. Ernzerhof, Generalized gradient approximation made simple, Phys. Rev. Lett. 77 (18) (1996) 3865–3868.
[44] D.J. Singh, Pseudopotentials and the LAPW Method, Kluwer, Boston, 1994.
[45] M.J. Frisch, G.W. Trucks, H.B. Schlegel, G.E. Scuseria, M.A. Robb, J.R. Cheeseman, J.A. Montgomery, T. Vreven, K.N. Kudin, J.C. Burant, J.M. Millam, S.S. Iyengar, J. Tomasi, V. Barone, B. Mennucci, M. Cossi, G. Scalmani, N. Rega, G.A. Petersson, H. Nakatsuji, M. Hada, M. Ehara, K. Toyota, R. Fukuda, J. Hasegawa, M. Ishida, T. Nakajima, Y. Honda, O. Kitao, H. Nakai, M. Klene, X. Li, J.E. Knox, H.P. Hratchian, J.B. Cross, C. Adamo, J. Jaramillo, R. Gomperts, R.E. Stratmannand, O. Yazyev, A.J. Austin, R. Cammi, C. Pomelli, J.W. Ochterski, P.Y. Ayala, K. Morokuma, G.A. Voth, P. Salvador, J.J. Dannenberg, V.G. Zakrzewski, S. Dapprich, A.D. Daniels, M.C. Strain, O. Farkas, D.K. Malick, A.D. Rabuck, K. Raghavachari, J.B. Foresman, J.V. Ortiz, Q. Cui, A.G. Baboul, S. Clifford, J. Cioslowski, B.B. Stefanov, G. Liu, A. Liashenko, P. Piskorz, I. Komaromi, R.L. Martin, D.J. Fox, T. Keith, M.A. Al-Laham, C.Y. Peng, A. Nanayakkara, M.

Challacombe, P.M.W. Gill, B. Johnson, W. Chen, M.W. Wong, C. Gonzalez, J.A. Pople, Gaussian 03 (2003).

[46] J. Haines, O. Cambon, E. Philippot, L. Chapon, S. Hull, A neutron diffraction study of the thermal stability of the α-quartz-type structure in germanium dioxide, Solid State Chem. 166 (2) (2002) 411–434.

[47] L. Levien, C.T. Prewitt, D.J. Weidner, The structure and elastic properties of quartz at pressure, Am. Mineral. 65 (9 &10) (1980) 920–930.

[48] K. Kihara, An X-ray study of the temperature dependence of the quartz structure, Eur. J. Mineral. 2 (1) (1990) 63–77.

[49] G.S. Smith, P.B. Isaacs, The crystal structure of quartz-like $GeO_2$, Acta Cryst. 17 (7) (1964) 842–846.

[50] H. Sowa, The oxygen packings of low-quartz and $ReO_3$ under high-pressure, Z. Kristallogr. 184 (3 & 4) (1988) 257–268.

[51] M. Iglesias, K. Schwarz, P. Blaha, D. Baldomir, Electronic structure and electric field gradient calculations of $Al_2SiO_5$ polymorphs, Phys. Chem. Miner. 28 (1) (2001) 67–75.

[52] X. Xue, M. Kanzaki, An ab initio calculation of $^{17}O$ and $^{29}Si$ NMR parameters for $SiO_2$ polymorphs, Solid State NMR 16 (2000) 245–259.